





Characteristics of long period microtremor and validation of microtremor array measurements in inland areas of China

CHE Ai-lan*  <http://orcid.org/0000-0003-3523-2832>;  e-mail: alche@sjtu.edu.cn

ZHANG Teng-yu  <http://orcid.org/0000-0002-5763-6400>; e-mail: xedwkhw@qq.com

FENG Shao-kong  <http://orcid.org/0000-0002-4171-9156>; e-mail: feng.sjtu@sjtu.edu.cn

* Corresponding author

School of Naval Architecture, Ocean and Civil Engineering, Shanghai Jiaotong University, 800 Dongchuan-Road, Shanghai 200240, China

Citation: Che AL, Zhang TY, Feng SK (2016) Characteristics of long period microtremor and validation of microtremor array measurements in inland areas of China. *Journal of Mountain Science* 13(11). DOI: 10.1007/s11629-016-3919-1

© Science Press and Institute of Mountain Hazards and Environment, CAS and Springer-Verlag Berlin Heidelberg 2016

Abstract: To study the characteristics of long period microtremor and applicability of microtremor survey, we have made microtremor observations using long period seismometers of the China's mainland from coastal cities like Shanghai and Tianjin through Beijing, Xi'an, to the far inland cities of Lanzhou and Tianshui. The observation shows that the level of power spectrum of long period microtremors reduced rapidly from the coast to the inland area. However, the energy of long period microtremors in Beijing, Xi'an, Lanzhou and Tianshui area are only approximately ten-thousandth to thousandth of that in Shanghai. Aiming at the complexity of the underground structure in the far inland, a series of underground structure models with different distributions were assessed using three-dimensional, dynamic finite element method (FEM) analyses. The results were used to evaluate microtremor survey methods and their limitations with regard to aggregate variability and thickness determinations. Multiple-wave reflections between layers with the change of underground structure distribution occurred, which have significant effect on the performance of the different field approaches. Information over a broad spectrum from which velocity-depth profiles were produced via inversion approaches. Neither the thickness nor the shear wave

Velocity V of the subsurface layer inversion results appeared over a large evaluation with increasing slope angle. In particular, when the angle of the model reached 45° , it could not be accurately evaluated using one-dimensional inversion methods. Finally, the array microtremor survey (AMS) was carried out in Shanghai City, China. Although AMS techniques do not have the layer sensitivity or accuracy (velocity and layer thickness) of borehole techniques, the obtained shear wave velocity structure is especially useful for earthquake disaster prevention and seismic analysis.

Keywords: Long period microtremor; Array Microtremor survey; Power spectrum; Inversion; S-wave velocity structure

Introduction

Microtremor observations, which include array microtremor survey (AMS) and horizontal-to-vertical spectral ratio microtremor (H/V) observation, are in expensive and non-intrusive methods to obtain the shear wave velocity or S-wave (V) profile. This important soil parameter represents the dynamic characteristics of a site (Arai and Tokimatsu 2005; Nakamura 1989; Okada 2003). S-wave velocity profiles play an important

Received: 2 March 2016
Revised: 20 July 2016
Accepted: 30 August 2016

role in the assessment of seismic hazard and simulation of strong ground motions (Horike 1985; Joyner 2000; Satoh et al. 2001). The single-station microtremor method is fast and cost-effective since it is based on a single-station measurement of ambient noise. The horizontal-to-vertical spectral ratio (H/V) is assumed to be related to the ellipticity of Rayleigh waves, which is either used as a direct measurement of the resonance frequency of a given site (e.g. Seht and Wohlenberg 1999; Parolai et al. 2001) or used in constraining the shear velocity profile in conjunction with surface wave dispersion information (e.g. Scherbaum et al. 2003; Arai and Tokimatsu 2005; Parolai et al. 2005). AMS involves the dispersion curve of Rayleigh waves obtained from ambient vibrations measured by an array of vertical sensors arranged in a specific shape (single/double triangle, etc.) on the ground surface. The method assumes that ambient vibrations mainly consist of surface waves, whose dispersion characteristics depend primarily on the shear wave velocities, density, and thickness of the different layers (Murphy and Shah 1988; Aki and Richards 2002).

In recent years, the redevelopment of metropolitan area and urbanization of the countryside has been accelerating in China. Characterized by high-rise buildings, long bridges, subway networks, and concentration of population, urbanization posed many new topics for earthquake disaster prevention. In particular, the analysis of seismic response of super high-rise buildings, super-large-bridges and other huge-scale structures that have long natural periods requires data regarding the deep geological structure down to the seismic base. On the other hand, after the great Wenchuan Earthquake in 2008 and Zhouqu Earthquake in 2010 (Huang 2009), both the government and people started to pay much closer attention to earthquake disaster mitigation. Since ground motion is determined by the seismic source and response of the site, any practical and effective earthquake disaster prevention program demands effective methods for site characterization, and the microtremor survey is expected to be important. AMS can be observed at any time and location, and the observation is much easier compared with other exploration methods. It causes no environmental or geological problems down to a depth of more than 100 m and can be inverted as

long as microtremors of required frequency range are observed (e.g., Horike 1985; Matsushima and Okada 1990; Kawase et al. 1998). A technique called frequency-wavenumber ($f-k$) spectrum method and spatial autocorrelation (SPAC) are used to obtain the Rayleigh wave dispersion curve from array microtremor (e.g., Horike 1985; Satoh et al. 2001a, b; Okada, 2003; Mundepi et al. 2010). The nature of Rayleigh wave dispersion curve for a site may be represented by the variation of the velocity with frequency, generally known as the phase velocity. Phase velocities of microtremors are estimated using the $f-k$ or SPAC methods and then V profiles for depths in the range of 100 m-3 km are obtained using array records of microtremors (Dutta et al. 2007; Boore and Asten 2008; Mundepi et al. 2010; Pilz et al. 2010; Wu and Huang 2012, 2013). V profiles are determined from inversion of surface waves dispersion (Ritzwoller et al. 2001; Shapiro and Ritzwoller 2002).

Ambient microtremors occur constantly as man-made and natural ground noise, which are caused by ocean wave activity, traffic, factories, wind, etc. The source of long period microtremors is mainly from ocean waves, storms, and other natural noise. The characteristics of long period microtremors are generally related to the property of the substructure and their sources. Their predominant frequencies are largely affected by the property of the substructure, and the influences of the amplitude are complicated. There are many application cases in Japan, Europe, America, and other countries surrounded by the sea (Apostolidis et al. 2006; Margaryan et al. 2009; Claprod, et al. 2009; EldeinZaineh et al. 2012). The characteristics of long period microtremors observed in inland area, which are far from the coast, should be paid special attention. However, either H/V spectrum or phase velocity by AMS is generally obtained by layered models based on one-dimensional Rayleigh wave problem (Yamanaka et al. 1994). Its reliability and suitability for slope or irregular models have not been clearly demonstrated. The geological structure of inland areas in China complicated. Therefore, a study on the characteristics of long period microtremors in the Chinese land is very important both theoretically and practically. In particular, it is necessary to investigate the applicability of microtremor surveys for testing and

analysis of the inland areas. We have started a research program on long period microtremors in China since 2009 (Sugiyama et al. 2009; Yu et al. 2011). The program consists of microtremor observations from the coast in the east to the inland area in the west (Shanghai, Tianjin through Beijing, Xi'an, Lanzhou and Tianshui cities), field test using H/V method, and AMS. The aim of this research program is to understand the characteristics of long period microtremors including variation of power spectrum from the coast to the inland region and based on field tests, to develop an observation and analysis method on site characterization to be used for China's earthquake disaster prevention program. In this paper, the level of microtremor amplitudes from the coast to the inland region is discussed. Aiming at the complexity of the underground structure in the far inland, especially in Lanzhou City, where a major river (Yellow River) running through the city causes complication of the geological structure, numerical simulation is conducted to evaluate microtremor survey methods and their limitations with regard to aggregate variability and thickness determinations.

1 Characteristics of Long Period Microtremor in China

1.1 Selection of Observation Sites

As shown in Figure 1, we selected Shanghai (38 sites, including Shanghai Jiaotong University area where also conducted array microtremor survey and east to west section area of Shanghai City) plus Tianjin (12 sites) in the coast, Beijing (4 sites) plus Xi'an (39 sites) in the middle, and Lanzhou (21 sites) plus Tianshui (34 sites) in the far inland as observation cities in order to examine the variation of microtremors from the coast to far inland. The observations were arranged in several rounds. The first round was carried out from March 18 to March 30 in 2009 (observed in Beijing and Tianjin cities), and the second round was carried out from May 1 to August 20 in 2010 (observed in Shanghai, Xi'an, Lanzhou and Tianshui cities) to observe the regional variation.

The distribution and physical properties of rock and soil in the observation site were

investigated by borehole sampling and geophysical exploration tests, as shown in Figure 2. It shows that the depth of subsurface soil layer is approximately 240 m with clay, silt, old clay, and fine sand in Shanghai observation sites. The sites are located on the leading edge southeast of the Yangtze River Delta, and the surface layer is of lagoon marsh landform; approximately 80 m with Q_2 (130,000-730,000 y), Q_3 (10,000-130,000 y), Q_4 (0-10,000 y) loess soil in Xi'an observation sites, and approximately 45 m with loess soil in Lanzhou observation sites. A major river (Yellow River) running through Lanzhou City, formed a long and narrow sites with the river in the middle and high mountains on both sides. With two mountains across Tianshui City in the north and south, the terrain landforms and geological structures are complex, as shown in Figure 1.

1.2 Instrument and Observation

Each set of instrument for microtremor measurement includes a long-period triaxial servo velocity sensor (VSE-311M), 24-bit analog-to-digital recorder with GPS time receiver (LS-7000), and 12 V car battery, as shown in Figure 3. This velocity sensor made by Tokyo Sokushin Co. Ltd., has a flat amplitude response from 0.05 to 70 Hz; its natural period is >10 s and sensitivity is 2V/kine. The digital recorder made by Hakusan Corp. has six Channels. The accuracy of the internal clock is within 1 ppm and is corrected by global positioning system (GPS) before each measurement. The positions of the sensors are determined using Trimble's GPS Pathfinder System receivers, which provide real-time submeter accuracy.

As shown in Figure 3, for most of the observation points, the seismometer is set up on a paved ground. If there is no paved ground suitable for observation, the natural ground is shaped flat and compacted hard before setting the seismometer. Furthermore, to prevent the influence of wind, when the set up is completed, the seismometer is covered by a transparent plastic case during observation and the case is firmly fixed by weights. The microtremor data are continuously recorded for approximately 12-25 h (25 h in Shanghai site, 13 h in Xi'an and Tianshui sites, and 12 h in Lanzhou site) during day time at a sampling frequency of 200 Hz.

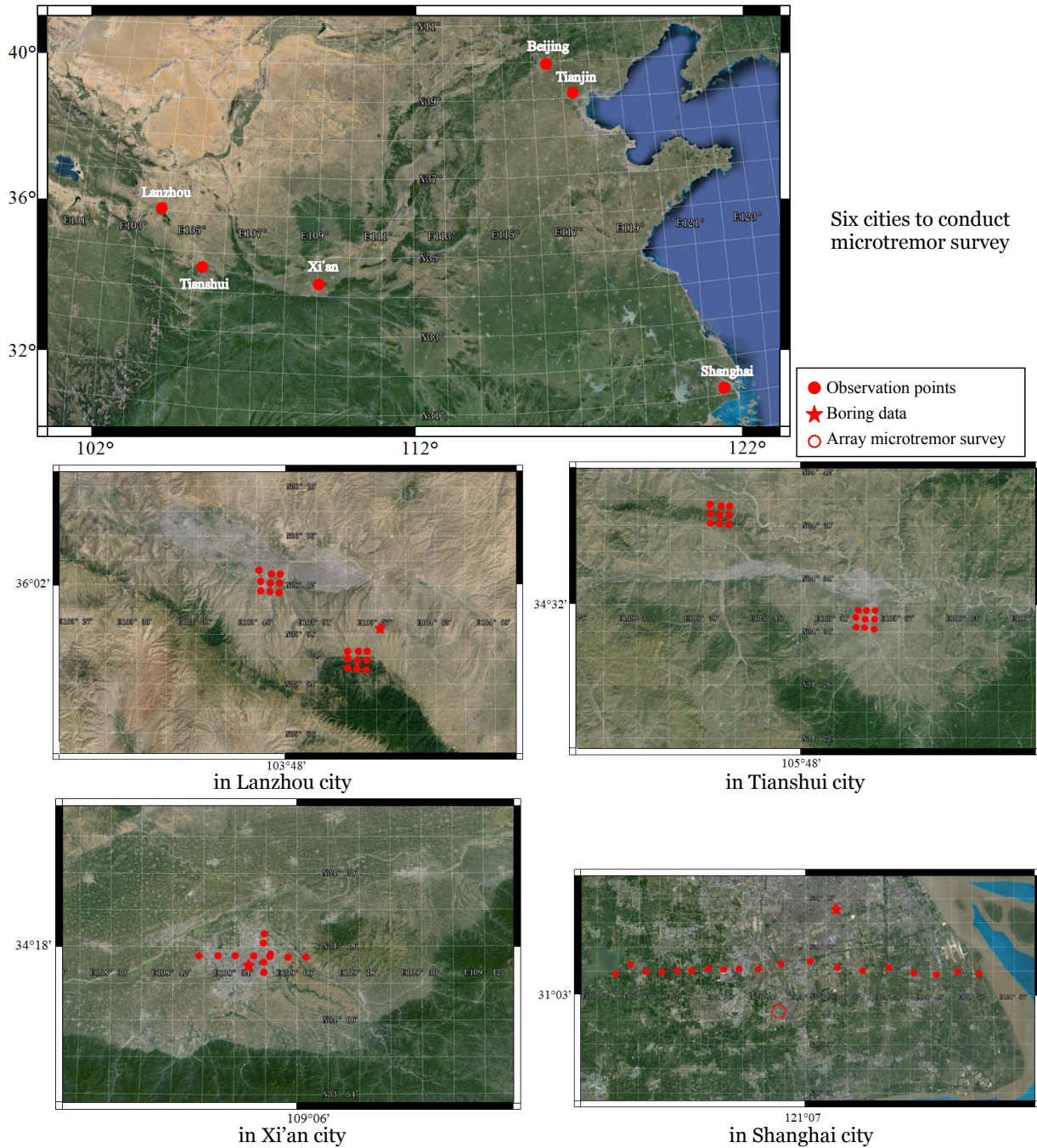


Figure 1 Observation sites in inland and coastal areas in China. In Beijing and Tianjin city, the observation areas are concentrated on one point.

1.3 Data analysis

Although the seismometer is portable and several minutes are needed for it to stabilize. For data processing, we discard the first 10 min of data without condition. Then, to ensure long period (10s) data and good resolution, we use a 327.68 s long-time window to cut the remaining data into time segments. The average amplitude and deviation of

each segment are analyzed, and all noisy segments are discarded. The time window with a 10% smooth taper is finely designed to reduce its effect on the spectrum estimated. The power spectrum of each segment is calculated by fast Fourier transform (FFT) and smoothed by a 0.05Hz Parzen spectral window. Finally, the power spectrum of the observed microtremor is calculated as the average of all live segments.

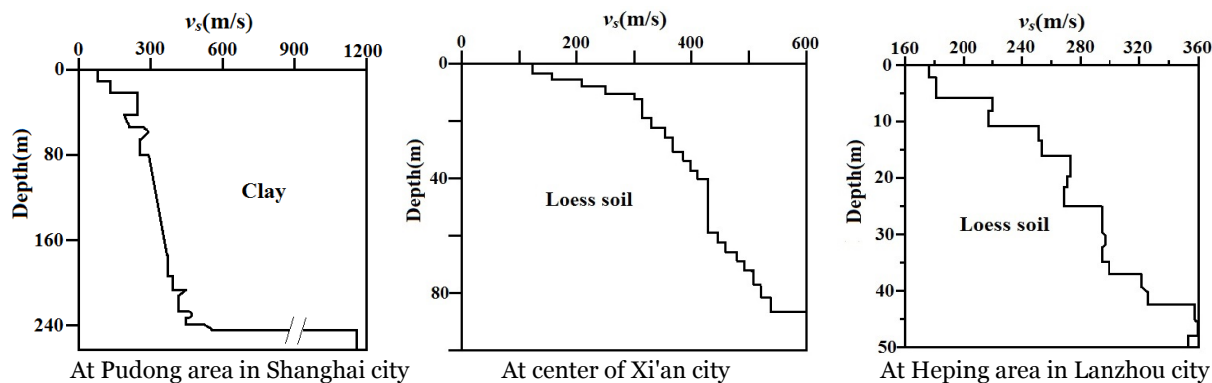


Figure 2 Borehole data in observation area.

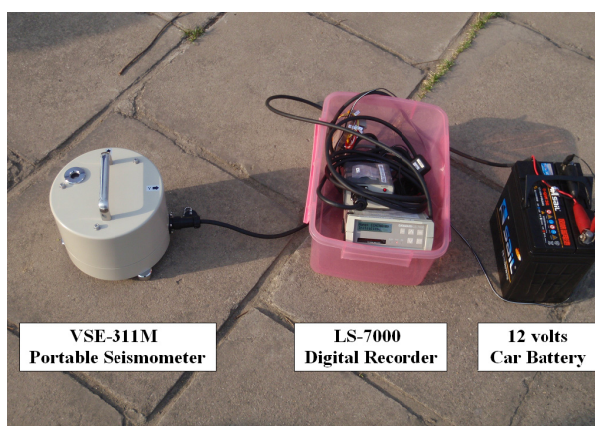


Figure 3 Configuration of observation system.

1.4 Power Spectrum and 13 h Variation

The result of over-13-h lasting observations in Shanghai (Shanghai Jiaotong University), Xi'an (Xi'an Jiaotong University), Tianshui (Tianshui Forestry School) and Lanzhou (Wuquanshan Park), and 1-h observations in Beijing (Beijing Jiaotong University) and Tianjin (Earthquake Administration of Tianjin Municipality) are shown in Figure 4 as variation of vertical component of power spectrum with time. As shown, for long period microtremors from 1 to 10 s, all the data have spectrum peaks of approximately 3-5 s. There is no obvious variation with time from the data in over-13-h of continuous observation. For Shanghai, Xi'an, Tianshui, and Lanzhou, the variation of long period microtremor from 1 to 10 s is in the order of 10^{-5} to 10^{-8} , 10^{-9} to 10^{-10} , 10^{-10} to 10^{-12} , and 10^{-9} to 10^{-12} cm^2/s , respectively.

1.5 Regional Variation

The level of power spectrum of microtremor

observed over the continent of China for long period microtremors in the range of 1-10 s is shown in Figure 5. As shown, although the level of power spectrum of microtremor observed are considerably different, they are more or less similar in shape. Among all the observation points in China, the power spectrum of long period microtremor in Shanghai is approximately in the range of 10^{-5} to 10^{-8} , the strongest one, and approximately in the range of 10^{-8} to 10^{-11} in Tianjin, the second strongest. Although Lanzhou and Tianshui in the far inland area are more than 1000 km from Beijing, the long period microtremor in these three cities are at the same level from 10^{-9} to 10^{-12} . The reasons for this could be the following: 1) the data were not observed on the same day, and 2) attenuation of long period surface wave is slight. As shown, long period microtremors observed in all other sites are only ten-thousandth of that in Shanghai. Furthermore, the spectrum in the far inland area of Lanzhou and Tianshui dropped down rapidly to approximately 1 Hz, forming a big trough. It can be assumed that the signal of microtremor is considerably weak and is beyond the limit of the measuring instrument.

2 Estimation of S-Wave Velocity Structure

The relationship between Rayleigh wave and subsurface structures is very complex. Therefore, the dispersion curve of the model can be calculated according to the matrix theory of layered medium, which approximates the subsurface model as a horizontal layered model (Haskell 1953; Knopoff 1964). In addition, the inversion analysis

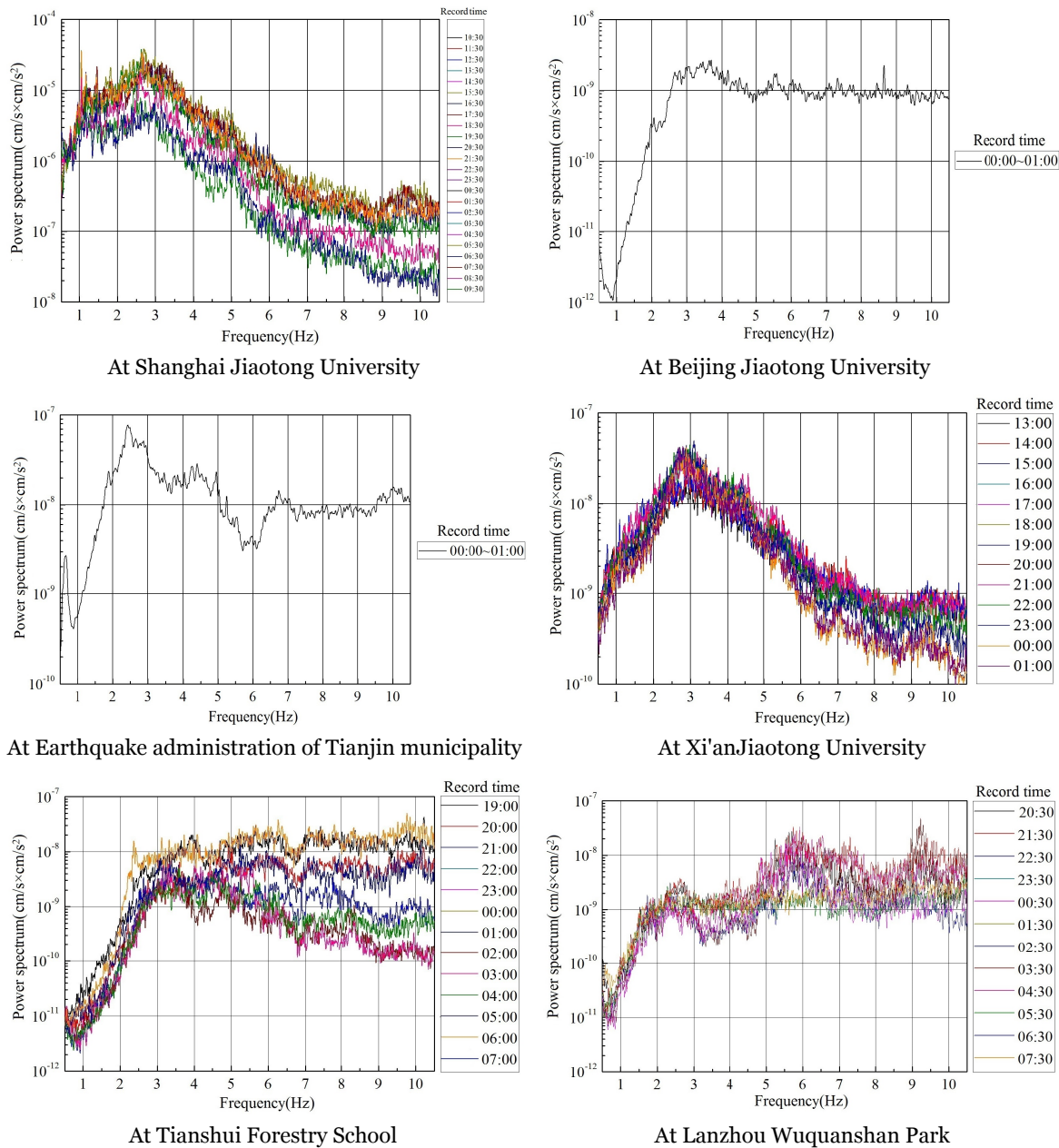


Figure 4 Power spectrum of Up-Down component at observation sites.

has high uncertainty, which generally requires certain known conditions. The underground structure in the far inland is complexity, which is difficult to simplify as layered model. Numerical simulation is applied by utilizing a series of models with different structures to evaluate microtremor survey methods and their limitations with regard to aggregate variability and thickness determinations.

Finite element method (FEM) dynamic

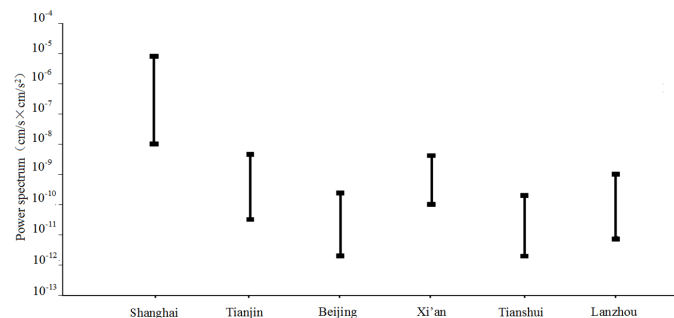


Figure 5 Level of power spectrum of microtremor observed over China for long period.

analyses are performed for wave propagations in underground structure models. Abaqus/Explicit is chosen as the solver for its transient dynamics simulation capabilities (Abaqus Explicit User Manual). For effectively simulating wave propagations in a 3D model, the size, degree of subdivision, and boundary conditions of the FEM models need to be optimized (Li et al. 2014; Rabczuk and Areias 2006).

2.1 3D Models and Parameters

Most cases of underground structure simulation in a large scale can be simplified as a layered model. For the complex geological structure in the far inland area, a series of semi-infinite 3D model underground structure with different distributions are assessed, as shown in Figure 6(a). The model is described by a rectangular coordinate system (x, y, z). The x-axis and y-axis constitute the model’s infinite dimension. The model is assumed to be symmetrical about the x-y planes. Because information about propagation in the unloaded model is required to determine whether adequate finite element discretization has occurred, free elastic waves in the infinite width models are discussed.

Numerical methods are used in the field of elastic wave modeling as follows:

- 1) FEM dynamic analyses are performed to describe the wave propagation.
- 2) The response of elastic waves with five types of models is discussed. As shown in Figure 6(a), the layered models are 3000×1500×600 m with dip angles of 10°, 20°, 30°, 45°. Hexahedron elements

are used to simulate the soil and rock mass. Considering the reflection and scattering in the boundary, the infinite element boundary condition is used at the base of the model. The infinite element is combined with the finite element. The dynamic response in near field region is simulated by the finite element and that in far field region is simulated by the infinite element. The boundary identification only removes the very high frequency noise and does not affect the effective periodic component of the elastic wave near the array area. Meshes with quadrilaterals and squares of 10 m side length were used to explore some qualitative features of the behavior of the model. This mesh model has 243,560 elements. The simulated three-component (two horizontal-EW, NS and one vertical-Up-Down) microtremor data are input on the side of the model.

3) An observed microtremor data is used as a slight disturbance from a far distance, which is observed on the bed rock in Shanghai area. First, a layered model of 6000×3000×600 m, which consists of clay, old clay, and bedrock as shown in Figure 6(b), is established to simulate the microtremor. The observed data is input in the z direction from 5km away from the side of numerical model, as shown in Figure 6(b). Then the responses in the side of the numerical model in three directions are obtained. Loading from a side of the model in three directions (Figure 6(a)), longitudinal waves (P) and shear waves (S) propagate radially outward along the radial direction of the hemisphere centered on the disturbed points. The Rayleigh wave (R) propagated in a cylindrical surface centered on the

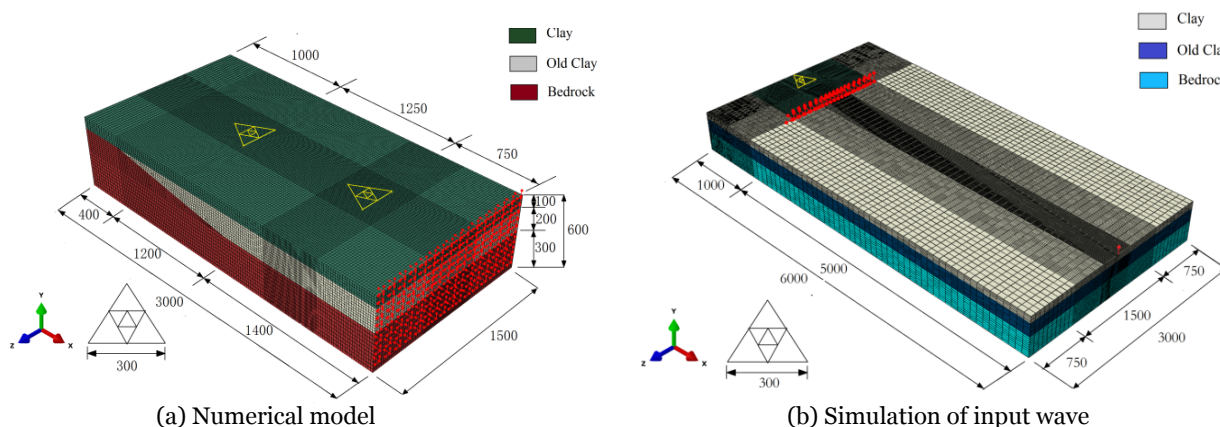


Figure 6 Mesh models used in the calculations (Dip angle is 10°, unit: m).

disturbed points as the column center. This wave consists of horizontal and vertical components, which compose an elliptical trajectory. Since the loading side is far from the observed array area, it can be assumed that long-period microtremors originated from far sources in various directions, and surface waves are dominant.

The material is considered as three layers composed of clay, old clay, and bedrock. The material parameters, as listed in Table 1, are chosen from the borehole data. Here, ρ is the density of the material, E is the modulus of elasticity, and μ is Poisson's ratio. The UD component of the observed microtremor data input on the side of the model in the vertical direction (Figure 6(a)) to simulate natural earth vibrations is observed on the bed rock in Shanghai area, as shown in Figure 7. Although the observations were conducted during quiet times, the recording is easily disturbed by environmental noise caused by traffic and construction works. Its predominant $f=0.7-0.8$ Hz, and duration $t=100$ s where $\Delta t=0.005$ s is used.

By using seismic arrays of ten seismometers placed on the surface of the model, the dynamic response of the observation points are obtained. Triangular arrays with 300 m side lengths are used at the slope site and layered site in order to resolve layers in the order 500 m depth. The center of the

Table 1 Mechanical parameters in the model

Material	E/MPa	$\rho/(\text{kg}/\text{m}^3)$	μ	$V(\text{m}/\text{s})$
Clay	335	1800	0.49	250
Old clay	582	1800	0.32	350
Bedrock	43000	2200	0.25	2800

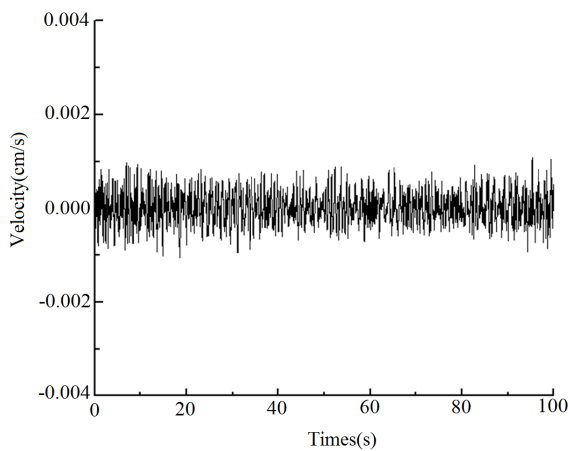


Figure 7 Up-Down components of observed microtremor data.

array is set as the depth where the sand layer is maintained at 100 m in different non layered models. Then, the distance from center of array to side of the model in the layered 10° , 20° , 30° and 45° model will be 600m, 1000m, 665m, 570m and 500m, respectively.

2.2 Numerical Results and Inversion

Array microtremor survey is divided into three steps:

(1) Array measurements: Multi observation points carried out by a number of high precision transducers are set on the ground according to certain geometric layout.

(2) Dispersion analysis: SPAC is used to obtain the Rayleigh wave dispersion curve (Aki 1957). The average values of the normalized autocorrelation function of the signal from the point and the center point of the circular observation array can be expressed as Eq.(1).

$$p(f, r) = \frac{1}{2\pi} \int_0^{2\pi} \frac{S(f, r, \theta)}{S_0(f, 0)S_r} d\theta = \frac{1}{2\pi} \int_0^{2\pi} \exp\left(\frac{2\pi f r}{c(f)}\right) \cos(\theta - \phi) d\theta = J_0\left(\frac{2\pi f r}{c(f)}\right) \quad (1)$$

where $S(f, r, \theta)$ is the cross spectrum of the signal from the center point and points j of the circular array; $S_0(f, 0)$ and $S_r(f, r)$ are the power spectrum of the signal from the center point and points j of the circular array; J_0 is a first-order Bessel function; θ is the incident angle of wave; $c(f)$, propagation velocity of wave; $\rho(f, r)$, autocorrelation function. For a particular frequency, the phase velocity is equal to what best fits a first-order Bessel function to the SPAC function.

(3) Inversion analysis: We conducted the inversion of the dispersion curves using a fully nonlinear procedure based on a combined approach, which employs a genetic algorithm technique with least-squares method (Yamanaka et al. 2005; Feng et al. 2001). The least-square method is usually required to have a high-precision initial model in order to get a stable solution. The genetic algorithm does not need the initial model, and all of the process involves forward calculation; therefore, the calculation process is stable. The first, step is to define the existence of a solution space, and then randomly generate N models. Afterward,

theoretical dispersion curves of each model are calculated. The advantages and disadvantages of each model are evaluated according to the difference between theoretical and observed values. According to a certain proportion, at which the quality model is retained, the selected model should be for crossover and mutation operation. A new generation is formed by combining the retained model and the model obtained by crossover and mutation processes. The process is repeated, and finally, the model is obtained when the difference between theoretical dispersion curve and the observed value is sufficiently small.

By FEM analysis the dynamic response of multi-observation points, which are set on the ground, are obtained. Based on phase velocity versus frequency showing the degree of fitness of the Bessel function to the SPAC function for a wide velocity and frequency range, the dispersion curves for different models is the peak (best fit), as shown in Figure 8. The dispersion curves for slope site from all four models are shown with the dispersion curve for the layered site. Similar distributions of dispersion curve appear in the 10° and layered site, and in the 20° and 30° sites. The dispersion curves for 10° and layered site show different from results for the 20° and 30° sites. The biggest difference is shown in nearby 1.0 Hz. In the 45° site, the distribution of the dispersion curve is relatively different from other sites.

Figure 9 is the shear wave velocity structure model of the geological structure estimated by phase velocity inversion for the measured site. The inversion has an estimated subsurface structure down to a depth of 600 m. The shear wave velocity of the last layer estimated is over 2000 m/s. Compared with the initial model (underground structure corresponding to the center of the array), V versus depth model in the inversion results agrees well with the profile of the layered model, especially in depth. The depth of clay layer obtained from inversion results shows good agreement with those of 10°, 20°, and 30° initial models. The depth of sand layer from inversion results shows over large evaluation, the error in depth reaches 33m, 52m, and 55m in 10°, 20°, and 30° sites, respectively. When the angle of the model reaches 45°, neither the depth nor the V of subsurface layer could not be accurately evaluated using the present analytical methods. The error in

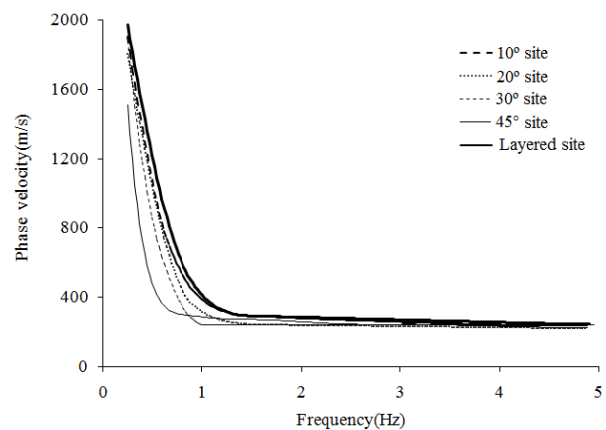


Figure 8 Dispersion curves calculated from array microtremor measurements.

depth of sand layer reaches 130m in 45° sites. Therefore, 2-D or 3-D subsurface structure should be considered in inversion analysis of complex subsurface structure model or multipoint simultaneous inversion should be used.

3 Application Test

To discuss the applicability of microtremor surveys in China, we have carried out a series of AMS field tests in Shanghai, Xi'an, Tianshui and Lanzhou cities. Figure 10 shows the field test of AMS at Minhang campus of Shanghai Jiaotong University located in south of Shanghai City, as shown in Figure 1. The array microtremor technique uses 15 units of 1-Hz geophones (VE-311M) arranged in a two-dimensional array. The triangular array, which consists of several embedded equilateral triangles, often provides good results with a relatively small number of geophones. With this array the outer side of the triangle should be at least as long as the desired depth of investigation (Feng et al. 2005). The data were observed using a triple concentric triangle (TCT) array, as shown in Figure 10, where $L=20, 50, 100, 250, \text{ and } 500$ m. Observation duration was set to 12 h. There is a known borehole data located at the north of the observed area whose distance is approximately 10 km. The depth of the bedrock is 320 m, and it is covered by clays, sands, silts and old clays. The array size was determined according to the borehole data.

The obtained energy spectrum and cross

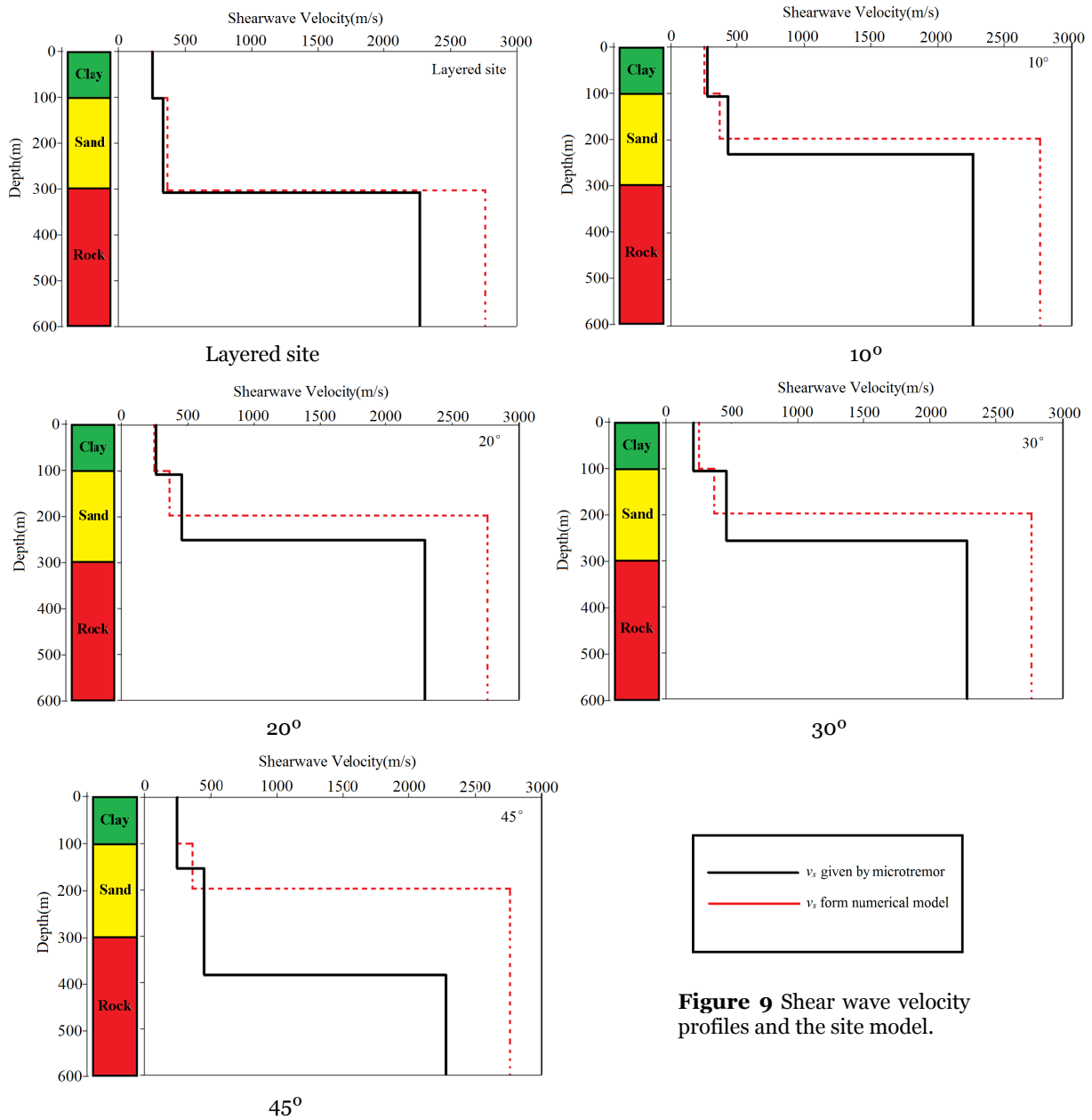


Figure 9 Shear wave velocity profiles and the site model.

spectrum are substituted into Eq.(1), then, the spatial autocorrelation coefficient for different lengths of the triangle array observations can be calculated, as shown in Figure 11. The propagation velocity of surface wave under different frequencies is calculated, and the dispersion curves are obtained. Figure 12 shows the phase velocity estimated from the microtremor using the SPAC method. The image shown is phase velocity versus frequency showing the degree of fitness of the Bessel function to the SPAC function for a wide velocity

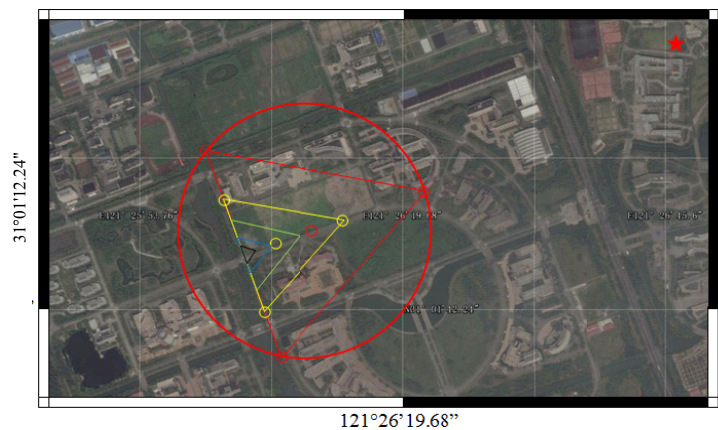


Figure 10 Layout of microtremor array.

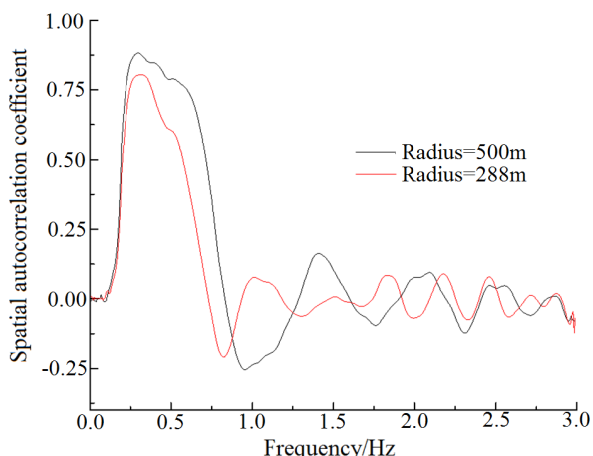


Figure 11 Spatial autocorrelation coefficient of microtremor observations.

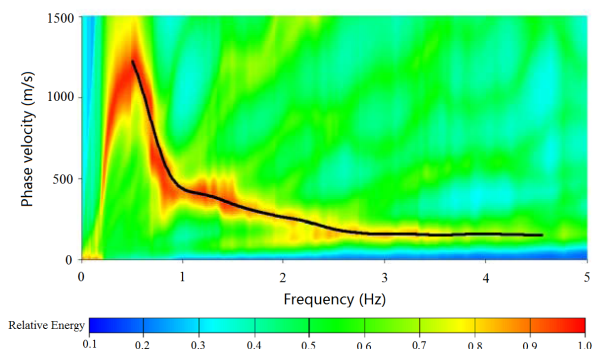


Figure 12 Phase velocity estimated from array microtremor survey for site at Shanghai Jiaotong University.

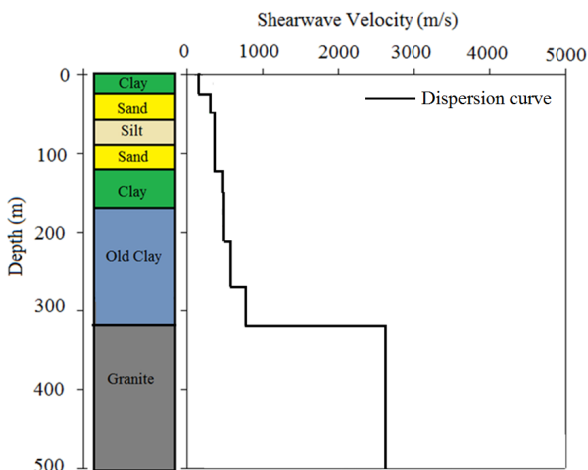


Figure 13 Structure model estimated by array microtremor survey.

and frequency range. The dispersion curve is the peak (best fit). The analysis estimates the phase velocity from 0.5 to 4.5 Hz successfully.

Figure 13 is the shear wave velocity structure

model of the geological structure estimated by phase velocity inversion. The inversion employs a combination of genetic algorithm and least-square technique. The inversion has an estimated subsurface structure down to a depth of 500 m. The shear wave velocity of the last layer estimated is over 2500 m/s. This is sufficient for site characterization for most civil engineering purpose. As shown, the depth of subsurface soil layer given by the survey agrees well with borehole data, which confirms the applicability of microtremor survey. In contrast to borehole measurement that is invasive and destructive, AMS is inexpensive and non-intrusive. In addition, it is relatively easy to obtain the necessary permits for AMS testing. Although AMS techniques do not have the layer sensitivity or accuracy (velocity and layer thickness) of borehole techniques, the average velocity over a large depth interval (i.e., the average shear wave velocity of the upper 1000m) is very well constrained.

4 Conclusions

We have carried out a series of long period microtremor observations and AMS from the coast to the far inland area to study the characteristics of microtremors over China. Conclusions of the research can be summarized as below:

(1) In coastal areas like Shanghai, the level of microtremor is the same as observed in Japan, inferring the applicability of microtremor survey. In inland areas, the level of long microtremor is only ten-thousandth of that in the coastal area; however, there is no obvious difference between inland areas (Beijing and Xi'an) and far inland areas (Lanzhou and Tianshui). In using long period microtremor for geological surveys in inland areas, continuous research should be done on the hardware system, observation method and data analysis method.

(2) Aiming at the complexity of underground structures in the far inland, numerical simulation was conducted to evaluate microtremor survey methods and their limitations with regard to aggregate variability and thickness determinations. Comparing the inversion results with the initial model, the depth of subsurface layer from inversion results shows over large evaluation with

increasing slope angle. When the angle of the model reaches 45° , neither the depth nor the V of subsurface layer could be accurately evaluated using the present analytical methods. The 2-D or 3-D subsurface structure should be considered in inversion analysis of complex subsurface structure model, otherwise, multipoint simultaneous inversion should be used.

(3) As a survey method using small equipment with no vibration, noise, or pollution, AMS was applied at sites in Shanghai City. Although AMS techniques do not have the layer sensitivity or

accuracy (velocity and layer thickness) of borehole techniques, the obtained shear wave velocity structure is especially useful for earthquake disaster prevention and seismic analysis.

Acknowledgments

This work was financially supported by the National Natural Science Foundation of China (Grant No. 11372180).

References

- Aki K (1957) Space and time spectra of stationary stochastic waves, with special reference to microtremors. *Bulletin of the Earthquake Research Institute* 35(3): 415-456.
- Aki K, Richards PG (2002) *Quantitative seismology*, 2nd edn. University Science Book.
- Apostolidis PI, Raptakis DG, Pandi KK, et al. (2006) Definition of subsoil structure and preliminary ground response in Aigion city (Greece) using microtremor and earthquakes. *Soil Dynamics and Earthquake Engineering* 26: 922-940. DOI: 10.1016/j.soildyn.2006.02.001
- Arai H, Tokimatsu K (2005) S-wave velocity profiling by joint inversion of microtremor dispersion curve and horizontal-to-vertical (H/V) spectrum. *Bulletin of the Seismological Society of America* 95(5): 1766-1778. DOI: 10.1785/0120040243
- Boore DM, Asten MW (2008) Comparison of shear-wave slowness in the Santa Clara Valley, California, using blind interpretations of data from invasive and noninvasive methods. *Bulletin of the Seismological Society of America* 98(4): 1983-2003. DOI: 10.1785/0120070277
- Claprod M, Asten Michael W (2009) Initial results from spatially averaged coherency, frequency-wavenumber, and horizontal to vertical spectrum ratio microtremor survey methods for site hazard study at Launceston, Tasmania. *Exploration Geophysics (Melbourne)* 40(1): 132-142. DOI: 10.1071/EG08106
- Dutta U, Satoh T, Kawase T, et al. (2007) S-wave velocity structure of sediments in Anchorage, Alaska, estimated with array measurements of microtremors. *Bulletin of the Seismological Society of America* 97(1B): 234-255. DOI: 10.1785/0120060001
- EldeinZaineh H, Yamanaka H, Dakkak R, et al. (2012) Estimation of Shallow S-Wave Velocity Structure in Damascus City, Syria, Using Microtremor Exploration. *Soil Dynamics and Earthquake Engineering* 39: 88-99. DOI: 10.1016/j.soildyn.2012.03.003
- Feng S, Sugiyama T, Yoshihiro S (2001) Estimating shear velocity using array-microtremor survey, Proceedings of The 4th international workshop on the application of geophysics to rock engineering, ISRM commission, pp89-98.
- Feng SK, Sugiyama T, Yoshihiro S (2005) Effectiveness of multi-mode surface wave inversion in shallow engineering site investigations. *Butsuri-Tansa* 58(1): 26-33. DOI: 10.1071/EG05026
- Joyner WB (2000) Strong motion from surface waves in deep sedimentary basins. *Bulletin of the Seismological Society of America* 90(6B): 95-112. DOI: 10.1785/0120000505
- Haskell NA (1953) The dispersion of surface waves on multilayered media. *Bulletin of the Seismological Society of America* 43: 17-34.
- Horike M (1985) Inversion of phase velocity of long-period microtremors to the S-wave-velocity structure down to the basement in urbanized area. *Journal of Physics of the Earth* 33(2): 59-96. DOI: 10.4294/jpe1952.33.59
- Huang RQ (2009) Research on development and distribution rules of geohazards induced by Wenchuan earthquake on 12th May 2008. *Chinese Journal of Rock Mechanics and Engineering* 27(12): 2585-2592.
- Kawase H, Satoh T, Iwata T, et al. (1998) S-wave velocity structures in the San Fernando and Santa Monica areas, Proceedings of the 2nd International Symposium on Effects of Surface Geology on Seismic Motions, Yokohama, Japan, 1-3 (2): 733-740.
- Knopoff L (1964) A matrix method for elastic wave problems, *Bulletin of the Seismological Society of America* 54(1): 431-438.
- Li XJ, Zuo YL, Zhuang XY, et al. (2014) Estimation of fracture trace length distributions using probability weighted moments and L-moments. *Engineering Geology* 168: 69-85. DOI: 10.1016/j.enggeo.2013.10.025
- Matsushima T, Okada H (1990) Determination of deep geological structures under urban areas using long-period microtremors. *Butsuri-Tansa* 43: 21-33.
- Margaryan S, Yokoi T, Hayashi K (2009) Experiments on the stability of the spatial autocorrelation method (SPAC) and linear array methods and on the imaginary part of the SPAC coefficients as an indicator of data quality. *Exploration Geophysics* 40(1): 121-131. DOI: 10.1071/EG08101
- Murphy JR, Shah HK (1988) An analysis of the effects of site geology on the characteristics of near-field Rayleigh waves. *Bulletin of the Seismological Society of America* 78(1): 64-82.
- Mundepi A K, Gallana-Merino J, Kamal J, et al. (2010) Soil characteristics and site effect assessment in the city of Delhi (India) using H/V and f-k methods. *Soil Dynamics and Earthquake Engineering* 30: 591-599. DOI: 10.1016/j.soildyn.2010.01.016
- Nakamura Y (1989) A method for dynamic characteristics estimation of subsurface using micro tremor on the ground surface. *Quarterly Report of RTRI* 30: 25-33.
- Okada H (2003) *The Microtremor Survey method*. Geophysical monograph series no 12. Society of Exploration Geophysicists with cooperation of Society of Exploration Geophysicists of Japan, Australian Society of Exploration Geophysicists.
- Parolai S, Piccozzi, M, Richwalski SM et al. (2005) Joint inversion of phase velocity dispersion and H/V ratio curves

- from seismic noise recordings using a genetic algorithm, considering higher modes. *Geophysical Research Letters* 32(1): 67-106. DOI: 10.1029/2004GL021115.
- Pilz, M., Parolai S, Picozzi M, et al. (2010) Shear wave velocity model of the Santiago de Chile basin derived from ambient noise measurements: a comparison of proxies for seismic site conditions and amplification. *Geophysical Journal International* 182(1): 355-367. DOI: 10.1111/j.1365-246X.2010.04613.x
- Rabczuk T, Areias PMA (2006) A new approach for modelling slip lines in geological materials with cohesive models. *International Journal for Numerical and Analytical Methods in Engineering* 30(11): 1159-1172. DOI: 10.1002/nag.522
- Ritzwoller MH, Shapiro NM, LeVhain AL, et al. (2001) The structure of the crust and upper mantle beneath Antarctica and the surroundings oceans. *Journal of Geophysical Research Solid Earth* 106(B12): 30645-30670.
- Satoh T, Kawase H, Iwata T, et al.(2001a) Estimation of S-wave velocity structures in and around the Sendai basin, Japan, using array records of microtremors. *Bulletin of the Seismological Society of America* 91(2): 206-218. DOI: 10.1785/0119990148
- Satoh T, Kawase H, Iwata T, et al. (2001b) S-wave velocity structure of the Taichung basin, Taiwan, estimated from array and single-station records of microtremors. *Bulletin of the Seismological Society of America* 91(5): 1267-1282. DOI: 10.1785/0120000706
- Scherbaum F, Hinzen KG, Ohrnberger M (2003) Determination of shallow shear wave velocity profiles in the Cologne, Germany area using ambient vibrations. *Geophysical Journal International* 152(3): 597-612. DOI: 10.1046/j.1365-246X.2003.01856.x
- Seht MI, Wohlenberg J (1999) Microtremor measurements used to map thickness of soft sediments. *Bulletin of the Seismological Society of America* 89(1): 250-259.
- Shapiro NM, Ritzwoller MH (2002) Monte-Carlo inversion for a global shear-velocity model of the crust and upper mantle. *Geophysical Journal International* 151: 88-105. DOI: 10.1046/j.1365-246X.2002.01742.x
- Sugiyama T, Feng SK (2009) Characteristics of long period microtremor over China continent, *Proceedings of 120th Society of Exploration Geophysicists of Japan conference, Sapporo, Japan (CD-Rom)*.
- Wu CF, Huang HC (2012) Estimation of shallow S-wave velocity structure in the Puli basin, Taiwan, using array measurements of microtremors. *Earth Planets Space* 64(5): 389-403. DOI: 10.5047/eps.2011.12.002
- Wu CF, Huang HC (2013) Near-surface shear-wave velocity structure of the Chiayi area, Taiwan. *Bulletin of the Seismological Society of America* 103(2a): 1154-1164. DOI: 10.1785/0120110245
- Yamanaka H, Takemura M, Ishida H et al. (1994) Characteristics of long-period microtremors and their applicability in exploration of deep sedimentary layers. *Bulletin of the Seismological Society of America* 84(6): 1831-1841.
- Yamanaka H, Motoki K, Fukumoto S, et al. (2005) Estimation of local site effects in Ojiya city using aftershock records of the 2004 Mid Niigata Prefecture earthquake and microtremors. *Earth Planets Space* 57: 539-544. DOI: 10.1186/BF03352589
- Yu k, Che AL, Feng SK (2011) Application on deep stratum of soil investigation using long-period microtremor. *Journal of Shanghai Jiaotong university* 45(5): 701-705. (In Chinese)